Memoirs of the Faculty of Engineering, Okayama University, Vol. 43, pp. 75-92, January 2009

Human Support Agent for Design and Diagnosis using Classifier System

Keita OHE *, Masami KONISHI and Jun IMAI
Division of Electronic and
Information System Engineering
Graduate School of Natural Science and Technology
Okayama University
3-1-1, Tsushima-Naka, Okayama, 700-8530

(Received November 26, 2008)

As is well known, an advanced knowledge and know-how are needed in the design and the diagnosis work. Further, human experts can cope with the recent trend of customers needs. Therefore, the design and the diagnosis work have been privately performed in the past, and its information cannot be shared. In addition, the number of experts is decreasing. It is a very important problem to maintain and to extend experts technologies having been built up. For the purpose, methods and systems for technical inheritance of the advanced techniques of the skilled engineers are needed to train the unskilled operators and also can assist skilled operators. In this research, attention is focused on the design of analog filter circuit. To attain the target, the circuit structural classifier system to support design work is developed. Furthermore, simulation technology for hot strip rolling mills based on distributed agents is presented aimed to develop tools for the diagnosis of hot strip rolling mills operation.

1 INTRODUCTION

As is well known, an advanced knowledge and know-how are needed in the design and the diagnosis work. Further, human experts can cope with the recent trend of customers needs. Therefore, the design and the diagnosis work have been privately performed in the past, and its information cannot be shared. It is difficult to bring down the skill technology as material object. Recently, the number of experts decreases. Therefore, it becomes an important problem to maintain and to extend experts technologies having been built up. For the purpose, methods and systems for technical inheritance of the advanced techniques of the skilled engineers are needed to train the unskilled operators and also can assist skilled operators. As the preparation, the design results and diagnosis results by experts are to be accumulated to make a database, and the system to share information is to be constructed. It is necessary to analyze the data in the database, and extract expert's knowledge. In this research, the efficiency improvement of design and an advanced diagnosis are achieved by discriminating the data with classifier system. In this paper, the design of filter circuit is treated as a example of the design, and diagnosis of hot strip mills operation is treated as a example of the diagnosis.

First, attention is focused on the design of analog filter circuit. To attain the target, the circuit structural classifier system to support design work is developed. This system involves three functions, optimization function, classification function, and retrieval of the related data base which supplies synergetic effects of these functions. The design of the filter circuit by Genetic Programming (GP) is achieved in the op-

*E-mail:ohe@cntr.elec.okayama-u.ac.jp

This work is subjected to copyright.
All rights are reserved by this author/authors.

timization function. The result designed by the optimization function is accumulated in the database. To organize it in the database, the circuit structure is classified in the circuit structure classification function. Self-Organizing Map (SOM) was applied to two or more circuits designed by the same design specification accumulated in the database, and the difference of the circuit was visualized. As a result, it becomes easy for the designer to refer the database, and it reflects on the design.

Next, simulation technology for hot strip rolling mills based on distributed agents is presented aiming to the diagnosis of hot strip rolling mills with controllers. In the operation of hot strip mills, human operators try to maintain rolling conditions in an appropriate situation. To help the operators, it is needed to build an intelligent rolling simulator which can check the whole rolling performances including control apparatus. To help human experts, it is necessary to simulate rolling phenomenon considering operating conditions in detail. It is also required to simulate results by changing control parameters. The quality of hot rolled product is greatly influenced by rolling velocity, hardness of the rolled material, aim gauge, rolling temperature and so on. A human expert senses these influences from his own experiences to cope with the effects. To automate expert's technology, it is necessary to simulate rolling phenomenon reflecting operating conditions in detail. So far, the simulator that used the deflection for control and partially expressed rolling existed. However, there are few simulators that precisely expressed the entire rolling. Then, the absolute value simulator used the nonlinear model was developed. Because the developed simulator is composed of the agent, the facilities and each controller can be exchanged. In this research, a virtual failure was caused preparatory for the operation support system, and the influence on the each facility was examined.

2 CIRCUIT STRUCTURAL CLASSIFIER SYSTEM

2.1 System Configuration

The composition of system is shown in Fig.1. The design support system is composed of the design support tool and the data base. The design support tool involves three functions, optimization, classification, and database. Specifications and circuit information for designed purpose are stored in the data base. The optimization function is improved reflecting the analyzed information in the database. Here, GP is used for the optimization of the circuit composition, and SOM is also used for the classification of the circuit structures.

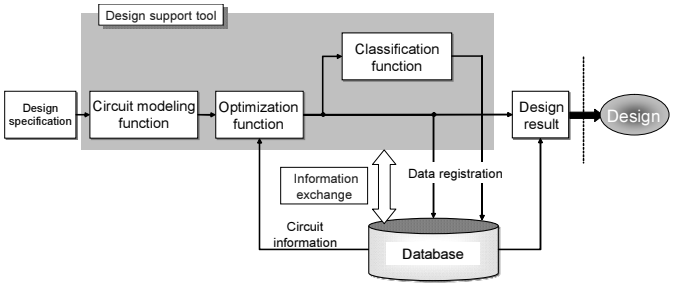

Fig. 1 System configuration

The flow of data in the design support system is described in Fig.1. First of all, the design specification is input considering characteristics assumed from the design object, a low-pass filter circuit, in this paper. Then, information and the operation instruction are transmitted to each simulator in the design support tool based on the design specification. The result is accumulated in the data base. After that, the accumulated data is analyzed in the data base. Finally, the analyzed result is considered or referred in the design support tool. As the result, it is expected that an efficient design support system with emergence is achieved.

2.2 Circuit Modeling

In this research, the circuit structure and its parameters are expressed by a tree structure for the design of the analog filter circuit. The turning point and the edge point of the tree structure are called a tree node, and connected point of the circuit is called a node only. The initial states of the tree structure are only two nodes of the input and the output. The nodes of various circuit elements and the connections are connected to the initial states of the tree structure, and the circuit is generated. Three kinds, the topology correction node, the element generation node and parameter calculation node, are defined as a node that composes the tree structure.

2.2.1 Topology Correction Node

Topology correction nodes for connection information are defined four kinds, series (SER), parallel (PAR), left node earth (GND1) and right node earth (GND2)), as shown in Figs.2 to 5. Each topology correction node has two arguments for node number, and makes a new node and a branch between nodes. The topology correction node or the element generation node can be connected to the lower node. The shape of the circuit generated by these combinations is determined.

- **SER** : SER symbol has nodes i and j as arguments, and generates node k between nodes i and j. Lower node of left side is passed nodes k and j, lower node of right side is passed nodes k and j as an argument. As a result, series branch is added between i and j.
- **PAR** : PAR symbol has nodes i and j as arguments, and passes nodes i and j to lower node of each side. As a result, parallel branch is added between i and j.
- **GND1** : GND1 symbol has node i and j as arguments. Lower node of left side is passed nodes i and *gnd*, lower node of right side is passed nodes i and j as an argument. As a result, ground branch of left side is added between nodes i and *gnd*.
- **GND2** : GND2 symbol has node i and j as arguments. Lower node of left side is passed nodes i and j, lower node of right side is passed nodes j and *gnd* as an argument. As a result, ground branch of right side is added between nodes j and *gnd*.

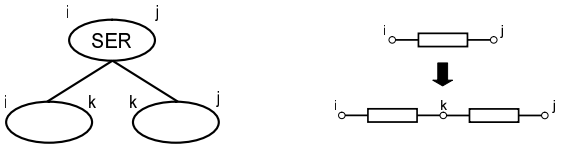

Fig. 2 Series connection

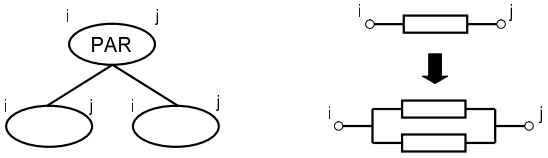

Fig. 3 Parallel connection

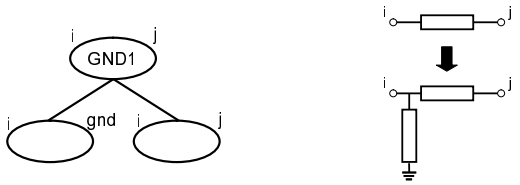

Fig. 4 Left side ground

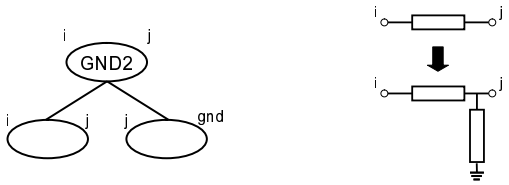

Fig. 5 Right side ground

2.2.2 Element Generation Node

Element generation node has two arguments for node number, and generates circuit elements like inductors and capacitors between nodes as shown in Fig.6. It is connected the parameter calculation node that decides the parameter of the circuit element generated by the element generation node as the lower node.

(a)Inductor(L)

(b)Capacitor(C)

Fig. 6 Element generation and parameter calculation node

2.2.3 Parameter Calculation Node

The parameter calculation node decides the argument value of the element that the element generation node of the upper node generates, and doesn't have the lower node. Therefore, the parameter calculation node becomes the terminal node of the tree structure. The parameter calculation node divides into p_1 and p_2 from side to side for the element generation node that is the

upper node as shown in Fig.6. The value of the element that the upper node generates is decided by $p_1 \times p_2$. Where, $p_1 \in parameter1$ and $p_2 \in parameter2$ are selected from the following value at random respectively.

$$parameter1 = \{1.0, 1.2, 1.5, 1.8, 2.2, 2.7, 3.3, 3.9, 4.7, 5.6, 6.8, 8.2\}$$
$$parameter2 = \{10^{-9}, 10^{-8}, 10^{-7}, 10^{-6}, 10^{-5}, 10^{-4}, 10^{-3}, 10^{-2}, 10^{-1}\}$$

The simple example of tree structure and circuit expressed by it are shown in Figs.7 and 8. However, the parameter calculation node is excluded.

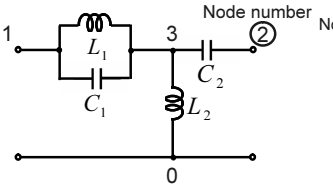

Fig. 7 Circuit structure

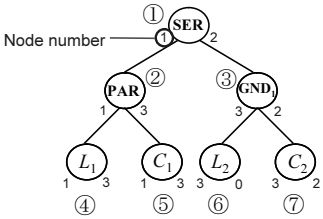

Fig. 8 Tree structure

2.3 Optimization Function

2.3.1 Circuit Design by Genetic Programming

Genetic programming is a method for searching of desired program by repeated application of operators such as mutation and crossover, and selection to the population of individuals that makes the program a gene. In this research, the solution was expressed by using the tree structures shown in Fig.8 in designing the circuit by GP. As a result, it becomes possible to treat the circuit with structures as a solution. The GP algorithm is very similar to usual GA. However, the following two points are different. One is that the solution is expressed by the tree structures. Another is to operate tree structures by genetic operators such as mutation and crossover. The tree structures change in small steps by applying those genetic operators. It is searched for the best tree structures by the selection according to the evaluation value and evolution.

2.3.2 Evaluation Method

The target of the filter circuit design is to design the circuit with the frequency response that satisfies the design specification satisfactory. The error of gain characteristics, the difference between targeted gain $g(\omega)$ and characteristic $f(\omega)$ of circuit designed by GP is evaluated by using the following evaluation functions. Gain characteristics are obtained by the circuit simulator.

$$I_1 = \sum_{i=0}^{n} (W(d(\omega_i), \omega_i) \times d(\omega_i)) \quad (1)$$
$$d(\omega_i) = |f(\omega_i) - g(\omega_i)| \quad (2)$$

Here, n is a number of samples, ω_i is a frequency, $f(x)$is an observation value in frequency x, $g(x)$is a target value (desired gain) in frequency x. $W(y, x)$is a weight function of error y in frequency x. For example, if the gain is ideal in sample point i, it is assumed W=0. It is assumed W=1 if it is within permissible limits, and W=10 if it violates limits. However, the value of W is suitably set by the emphasized part of the frequency response. When it was not possible to analyze it with the circuit simulator, it was given 10^6 as the worst evaluation value.

GP is a technique that the set passes the generation and the individual repeats crossover. As a result, it is known that the phenomenon of size about the tree structure of the individual explosively increases. This phenomenon is called bloat. In this research, the bloat problem is connected directly with the complexity of the designed circuit. In the filter circuit design, it is not an ideal circuit when the circuit scale is too large even if the frequency response is ideal. Then, it was adopted the method for adding the number of nodes of tree structures designed by GP to the evaluation function to avoid the bloat problem.

It is assumed that the number of nodes of circuits generated with a certain tree structure is N, and the number of elements was n. Number N of nodes is proportional to number n of elements ($N \propto n$). At this time, the evaluation value is calculated by the following equation.

$$I_2 = k_1 N^{k_2} \quad (3)$$

Where, k_1 and k_2 are coefficients.

In addition, the evaluation about attenuation slope has not been taken in previous studies. However, attenuation slope in the frequency characteristic greatly influences the performance of a filter circuit. In this research, attenuation slope of the circuit designed by GP is added to the evaluation function. The evaluation value about attenuation slope is calculated by the following equation.

$$I_3 = k_3 \frac{G_{f_2} - G_{f_1}}{\log_{10} f_2 - \log_{10} f_1} \quad (4)$$

Where, k_1 is a coefficient, f_1 and f_2 are sample frequencies, G_{f_2} and G_{f_1} are the gain at sample frequencies.

The evaluation function finally obtained is the following expressions which combine Eqs.(1) and (3).

$$\begin{aligned} &\min I; \\ I &= I_1 + I_2 + I_3 \\ &= \sum_{i=0}^{n} (W(d(\omega_i), \omega_i) \times d(\omega_i)) \\ &\quad + k_1 N^{k_2} + k_3 \frac{G_{f_2} - G_{f_1}}{\log_{10} f_2 - \log_{10} f_1} \end{aligned} \quad (5)$$

The value of I_1 can be expected from how to decide the value of W in advance. k_1 and k_2 of Eq.(5) are adjusted for I to have a profound effect on when the value of I_1 has approached the ideal value.

2.3.3 Circuit Design Algorithm

In this research, the circuit is designed by GP. The design procedure by GP is shown as follows.

STEP1 Design Specification
Ideal characteristics of frequency and permitted region are determined by considering the realistic problem from desired specification. The design specification is input.

STEP2 Generation of Initial Set
N individuals with the tree structure are generated at random, and initial set $P(0)$is set. A certain number of individuals lead to a global search in GP. Moreover, repeat times T, final generation, is set.

STEP3 Evaluation
The fitness of each individual is calculated. The fitness is quantitatively an evaluation how the individual has adapted to the environment. In this research, it is shown that the larger the fitness is, the higher the performance as the filter circuit is. The fitness is determined by using Eq.(5).

STEP5 Convergence Test
If it is $t = T$, the calculation is ended. The individual of the maximum fitness that has been obtained so far is assumed to be a suboptimal solution, and the circuit configuration is output. Otherwise, the inheritance operation is added to the individual set.

STEP4 Selection
It is easy to be selected in the solution with good evaluation value. In this research, roulette wheel selection is used together with the elite preservation selection. The elite selection is sequentially selected from the solution with good evaluation value. Afterwards, all the solutions of the remainder are selected by roulette wheel selection. The roulette wheel selection is a technique which the solution is selected by the ratio proportional to the evaluation value. When the evaluation value of each solution is assumed $f_i (i = 1, 2, \cdots, N)$, probability p_j of solution j is selected becomes the following expression.

$$p_j = \frac{f_j}{\sum_{i=1}^{n} f_i} \quad (6)$$

The solution selected by the elite preservation selection is not an object of genetic operators.

STEP6 Crossover
The node is selected at crossover rate p_c from among all nodes other than the root of the individual i and j. Selected nodes are exchanged, and partial trees of the node are exchanged together at the same time. Non-selected node is not exchanged, and copied with a partial tree. The appearance of crossover is shown in Fig.9.

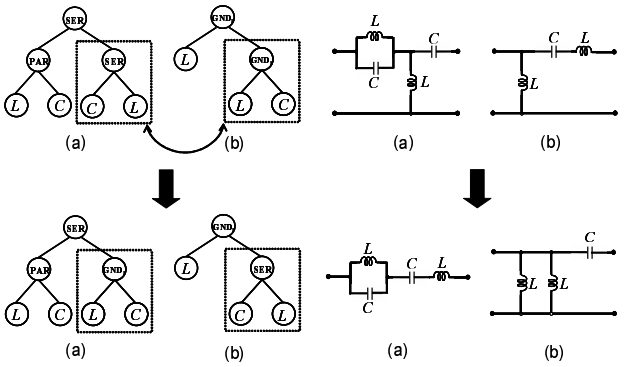

Fig. 9 Crossover

STEP7 Mutation
In the mutation in GP, the mutating node is selected to one individual at random. It replaces selected node with the node generated with mutation rate p_m at random. Here, if the selected node is a terminal node, the mutating node is made a terminal node. Oppositely, if the selected node is non-terminal node, the mutating node is made non-terminal node. That is, if the mutating node is non-terminal node, the symbol of the

mutation point is changed to the same kind of symbol. If it is a terminal node, the argument value of the symbol of mutation point is changed. Next generation set $P(t+1)$is generated after the mutation operation and it returns to STEP3.

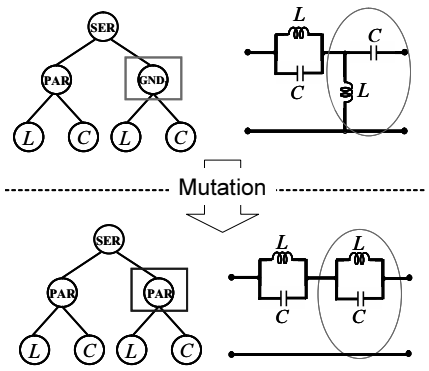

Fig. 10 Mutation

2.4 Classification Function

2.4.1 SOM

The process which the designer classifies the circuit structure is highly sophisticated. It is impossible to express its process mathematically. Here, SOM which is a simple model to express the information processing of the brain was used to classify the circuit structures. SOM proposed by Kohonen is composed as shown in Fig.11.

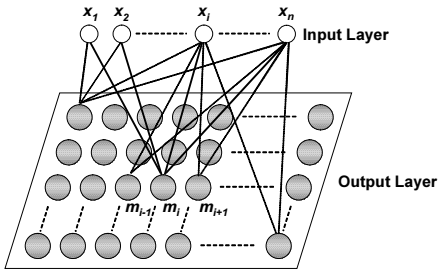

Fig. 11 Structure of SOM(two-dimensional SOM)

In basic learning algorithm of SOM[5], the vector is updated to the unit located in victor unit m and its neighborhood by the following expression. The update rule of SOM vector is shown below.

$$w_i(t+1) = w_i(t) + \eta(t)[x(t) - w_i(t)] \quad (7)$$

$$N_{j^*}(t) = [N_{j^*}(0)(1 - t/T)] \quad (8)$$

$$\eta(t) = \eta(0)(1 - t/T) \quad (9)$$

Here, x is the maximum integral value that doesn't exceed x. Constant $N_{j^*}(0)$between the input layer and the output layer sets a positive integral value. S_{j^*} is sets of $9(= 3 \times 3)$ units that surround victor unit K_{j^*} when $N_{j^*}(t) = 1$. $\eta(t)$ becomes an update rate that is smaller than the victor unit for the neighborhood units other than the victor. That is, it becomes small for the unit at a position away from the victor unit. The Euclid distance between the input vector and the uniting load vector to the output layer is calculated from Eq.(10).

$$d_j = \sqrt{||x(t) - w_j(t)||^2} \quad (10)$$

Using d_j values, output layer is determined. As the result of learning, the degree of similarity between input data is corresponding to the distant relation on the lattice in the output layer.

2.4.2 Classification of Circuit Structures

Circuit structures are classified with SOM by using the amount of characteristic information of the circuit obtained from node information of the tree structure. It allows to project multi-dimensional information to the lower dimensional level. That is, it is possible to classify circuit structures projecting to the tree structure that is a multi-dimensional structure to two dimensions, and calculating the degree of similarity for each input.

The input is the summation of node information in the tree structure. The circuits with simple structures shown in Figs.12 and 13 are considered.

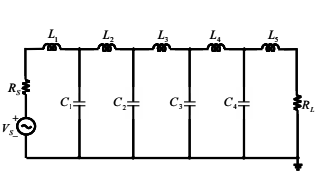

Fig. 12 Case1 circuit

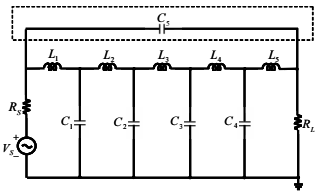

Fig. 13 Case2 circuit

Table 1 shows the sum of each node information that composes the circuit shown in Figs.12 and 13.
Here, the input values to SOM are used transforming to normalized values. A greatly different nodes are PAR and GND_2 in information on Case1 and Case2 as shown in Table 1. Thus, a structural difference shows node information of each circuit.

Table. 1 Node information

	SER	PAR	GND_1	GND_2	L	C
Case1	4	0	3	1	5	4
Case2	4	1	4	0	5	5

2.4.3 Classification Case

It was confirmed that the circuit structure was classified by SOM through classification case. The classified circuits are shown Figs.12 and 13, and similar to each circuit. The classified circuits are shown in the following table.

Table. 2 Input to SOM

	SER	PAR	GND_1	GND_2	L	C
Case1	4	0	3	1	5	4
Case2	4	1	4	0	5	5
Case3	4	1	4	0	5	5
Case4	4	1	4	0	5	5
Case5	4	1	4	0	5	5

Case2 is a similar circuit to Case1, and Case4 and Case5 are similar circuits to Case3. The target of classification is to classify it into two clusters of Case1, 2, and Case3, 4 and 5. The learning condition is given in Table 3.

Table. 3 Learning condition

Learning times	1500[-]
Learning rate	0.5[-]
Neighborhood radius	5[-]
Map size	10×10[-]
Neighborhood function	bubble

The result of classifying the circuit structure is shown in Fig.14 by using the learning condition given in Table 3. Case2 is a similar circuit to Case1, and Case4 and Case5 are similar circuits to Case3. The target of classification is to classify it into two clusters of Case1, 2, and Case3, 4 and 5. The learning condition is given in Table 3. From Fig.14, the circuit similar to case1 was classified into the node (2, 3), and the circuit similar to case2 was classified into the node (9, 6). It was classified into two clusters of Case1, 2, and Case3, 4 and 5. Thus, the circuits with different structure could be classified by inputting node information.

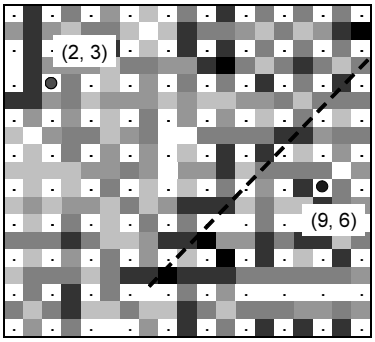

Fig. 14 Classification result

2.5 Application of Database

The objective of classification of circuit structures is mainly to arrange the design result in the database. The data of the design result by GP and classification result of circuit structures are accumulated in the database. The accumulated data is node information of tree structures of design result by GP and partially structural information. Partial structural data plays the role of the arrangement of the database. Here, the method of applying node information by accumulating in the database is shown below. If design result is divided into three nodes, there are 144 kinds of node. All node information that composes the tree structure was accumulated. A example of use frequency is shown in Fig.15. It is shown accumulation of the design result

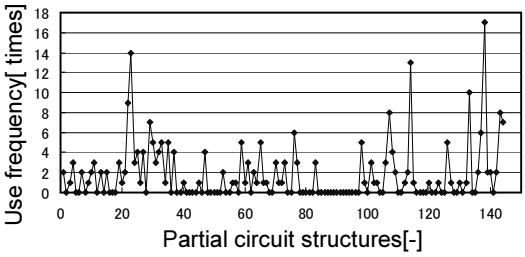

Fig. 15 Use frequency of partial structures

by GP 20 times.

There is a large difference in the use frequency of partial structures shown in Fig.15. Then, probability density function $p(i)$ to a partial circuit structure i is defined.

$$p(i) = \frac{q_i}{P} \tag{11}$$

Here, q_i is use frequency of a partial circuit structure i,

and P is sum of the use frequency of the partial circuit structure. An initial solution is generated by using this probability density function $p(i)$. That is, it meets to limiting the solution space.

2.6 Numerical Experiment

2.6.1 Design Specification of LPF

The low-pass filter(LPF) circuit where the boundary of the passband and the cutoff area is 1[kHz] was designed. As for the design specification, the passband of an ideal characteristic is [0, 1000] where desired gain is 0[dB]. The gain in other bands is less than -120[dB]. The allowable range was set in all bands. It is within $\pm$ 0.6[dB] in the passband, and below 0[dB] in 3[kHz] and under, and below -50[dB] in other bands.

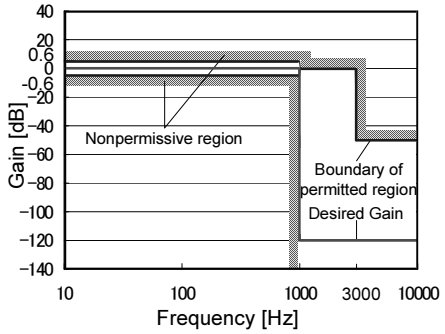

Fig. 16 Design specification

The observation point are taken at 101 frequencies with equal increment in logarithmic scale between 10[Hz] and 10[kHz]. A weight is determined from the difference between the response and the aimed value, and the fitness is calculated in each sample point. Weight W is determined as follows.

In the passband,

- If the gain is 0[dB], difference $d(f_i)$ is 0.0.
- If the gain is within $\pm$ 0.6[dB], weight $W(d(\omega_i), \omega_i)$ is 10.0.
- In forbidden region otherwise, weight $W(d(\omega_i), \omega_i)$ is 100.0.

In other bands,

- If the gain is under -120[dB], difference $d(f_i)$ is 0.0.
- If the gain is under permitted region, weight $W(d(\omega_i), \omega_i)$ is 1.0.
- In forbidden region otherwise, weight $W(d(\omega_i), \omega_i)$ is 10.0.

The parameter of GP is shown in table 4. The coefficient k_1 is $\frac{\log_{10} f_i}{2 \cdot 30}$, k_2 is 1.5, and k_3 is 10.

Table. 4 Each parameter of GP

Parameter	Value
Individual$N$	3000[-]
Generation$T$	100[-]
Crossover ratep_c	90[%]
Mutation ratep_m	10[%]

The tree structure of an initial individual is generated at random. However, even if a large individual is composed first, it is not effective. Then, the limitation of six in depth was set in the maximum. The necessity in an initial set is parts of the tree structure composing the individual.

2.6.2 Optimization Function

The utility of the filter circuit design by optimization using database information was examined. Two evaluation indices are selected. One is an error between the ideal gain characteristic and the designed circuit, and the other is a number of circuit elements. The design result with or without database is shown below. The changes of the evaluation values are shown in Fig.17. The best result of design trials of twenty times is compared with desired gain in Fig.18.

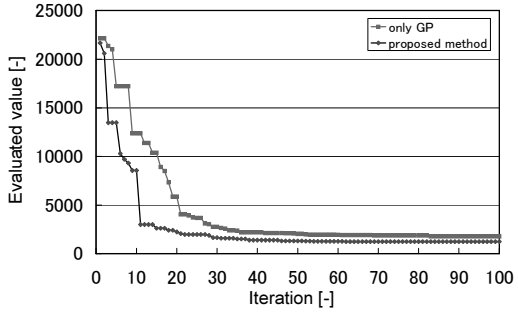

Fig. 17 Changes of evaluation value

It can be confirmed that the evaluation value is improved with iterations from Fig.17. Furthermore, the

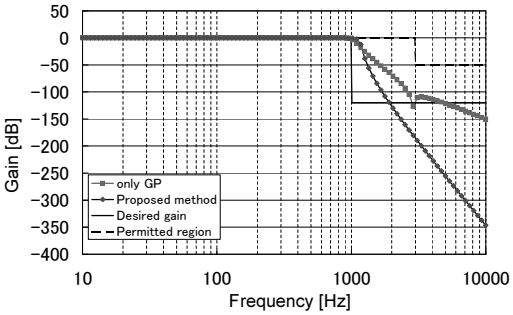

Fig. 18 Frequency characteristic

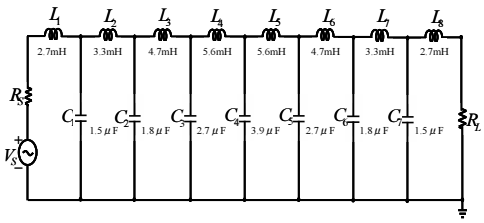

Fig. 19 Designed circuit by GP

filter circuit that satisfied the design specification was able to be designed from Fig.18. Two interesting conclusions were obtained. First, the solution has been improved by using data base information. Moreover, it has been understood that emergence becomes weak when database information is used. Finally, solution converged to the general and high-dimensional filter circuit.

2.6.3 Classification Function

It designed twenty times by GP in a numeric experiment. That is, twenty circuits are accumulated in the database. The result that each circuit is projected on the map to two dimensions is shown. The result of classifying the circuit structure is shown in Fig.20 by using the learning condition given in Table 3.

It is classified intensively to the top-left and the bottom-right part in Fig.20. Here, the circuit of (2, 3) on the upper left and (8, 7) on the lower right are shown below as the representative point.

As for the circuit in the top-left part, the composed number of elements is small with 8 pieces, and the circuit structure is also simple. And as for the circuit in the bottom-right part, the composed number of elements is large with 15 pieces, and the circuit structure

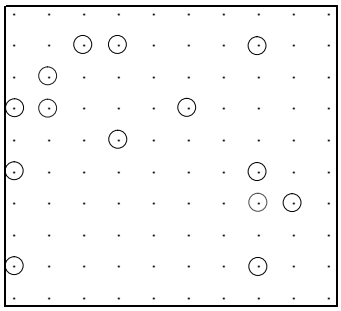

Fig. 20 Classification result

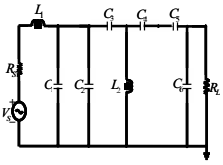

Fig. 21 Top-left part circuit

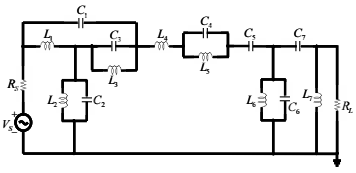

Fig. 22 Bottom-right part circuit

is also complex. It is confirmed that the classification result greatly influences a numerical of element and structural complexity. Thus, it is shown that the database is arranged by classifying the circuit structure.

3 AGENT BASED DIAGNOSIS SYSTEM OF HOT STRIP MILLS

In this paper, the simulation technology for hot strip mills is mainly described. The diagnosis system using the simulator is proposed. A virtual failure is caused by the simulation in preparation for the diagnosis system.

3.1 Agent based Simulation Model

Construction of the agent based simulation model is shown in Fig.23.

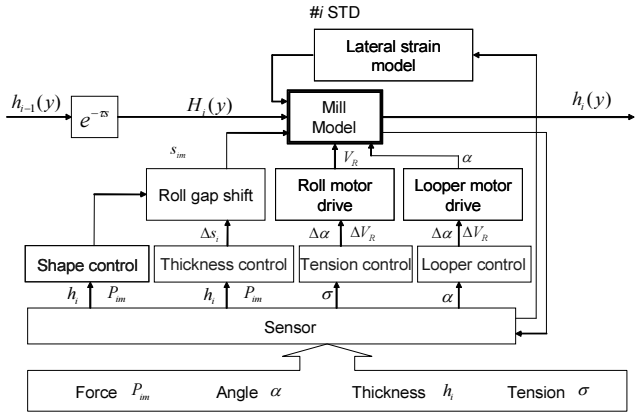

Fig. 23 Agent based simulation model

The simulation model for rolling mill is composed of mill models with lateral roll deformation. Mill model has a function of reproducing rolling phenomenon. Inputs to the mill model are given by entry thickness, outputs form mill drive motor, looper drive motor and output of mill controllers. As for the control systems, shape control, thickness control, tension control, and looper control are provided. The data measured by various sensors are input to these control systems, and the amounts of the control are calculated. All of these subsystems and controllers are provided with agent functions. These agents automatically output necessary control values judging from input data.

3.2 Mathematical Model for Hot Rolling Mills

In this research, the rolling phenomena was reproduced by each agent model. In the following, the mathematical models for each agent and that of hot strip rolling will be shown.

3.2.1 Mill Agent Model

It is shown the concept of mill agent in Fig.24. The

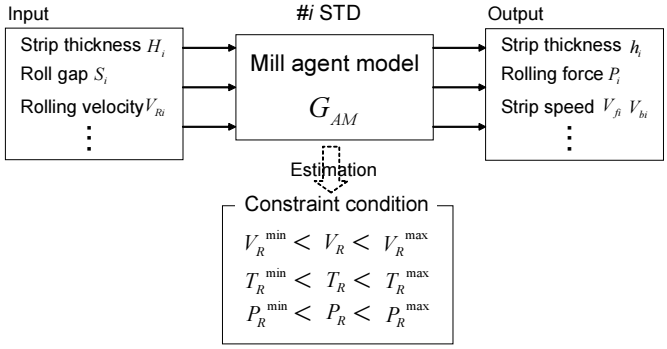

Fig. 24 Mill agent model

mill agent is a model which outputs the rolling result autonomously satisfying various constraints according to setting values of rolling conditions. The mill system treated in this paper consists of three stands and two looper facilities. It is shown relations between entry strip thickness $H(t)$, exit strip thickness $h(t)$, roll gap $s(t)$, and rolling force $P(t)$ that are basic variables of mill system shown in Fig.25.

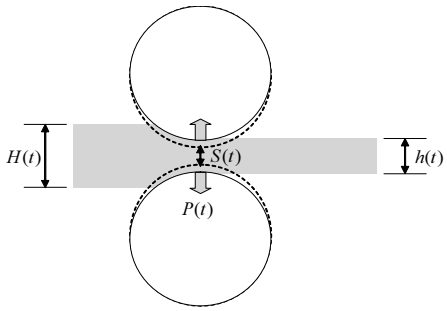

Fig. 25 Fundamental relation of rolling

The fundamental equations for the hot rolling process

are described as follows.

$$P_i = bK_{fm}\sqrt{R'_i(H_i - h_i)}Q_i \quad (12)$$

$$Q_i = \sqrt{\frac{h_i}{H_i - h_i}}\{\frac{\pi}{2}\arctan\sqrt{\frac{H_i - h_i}{h_i}} - \sqrt{\frac{R'_i}{h_i}}\ln\frac{h_{\phi i}}{h_i} + \frac{1}{2}\sqrt{\frac{R'_i}{h_i}}\ln\frac{H_i}{h_i}\} - \frac{\pi}{4} - \frac{\sigma_b}{K_{fm}} \quad (13)$$

$$h_{\phi i} = \frac{h_i}{\cos {F_i}^2} \quad (14)$$

$$F_i = \frac{1}{2}\arctan\sqrt{\frac{H_i - h_i}{h_i}} - \frac{\pi}{8}\sqrt{\frac{h_i}{R'_i}}\ln\Big(\frac{H_i}{h_i}\Big) - \frac{1}{2}\sqrt{\frac{h_i}{R'_i}}\frac{\sigma_b}{K_{fm}} \quad (15)$$

$$R'_i = R_i\Big(1 + \frac{cP_i}{b(H_i - h_i)}\Big) \quad (16)$$

$$\phi_i = \sqrt{\frac{h_i}{R'_i}}\tan F_i \quad (17)$$

$$f_{si} = \frac{1}{2}{\phi_i}^2\Big(\frac{2R'_i}{h_i} - 1\Big) \quad (18)$$

$$f_{bi} = \frac{h_i}{H_i}(1 + f_{si}) - 1 \quad (19)$$

$$h_i = s_i + \frac{P_i}{M_i} \quad (20)$$

Here, P_i, K_{fm}, H_i, h_i, s_i, f_{si}, f_{bi} are rolling force, flow stress, entry strip thickness, exit strip thickness, roll gap, forward slip ratio, respectively. M_i is mill modulus, and subscript i denotes i^{th} stand. Using f_{si} and f_{bi} given by solutions of above equations, exit strip speed v_{fi} and entry strip speed v_{bi} can be obtained as follows.

$$v_{fi} = V_{Ri}(1 + f_{si}) \quad (21)$$

$$v_{bi} = V_{Ri}(1 + f_{bi}) \quad (22)$$

Where, V_{Ri} is the rolling velocity of i^{th} stand.

3.2.2 Tension/Looper Agent Model

Tension/looper agent are agents which determine looper angle and looper drive torque autonomously when set values of each rolling conditions are input. Tension/looper system is shown in Fig.26. The equation of looper movement after a looper roll and rolled material come in contact is given as follows.

$$J\ddot{\theta} = T_{Lref} - \delta\{K_1(\theta)\sigma + K_2(\theta)\} - K_3(\theta) - D\dot{\theta} \quad (23)$$

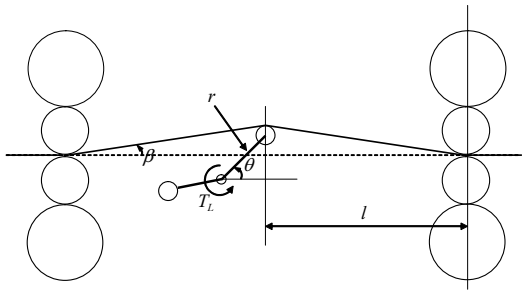

Fig. 26 Looper system

Where, K_1 is torque by the tension, K_2 is torque by strip weight, and K_3 is torque by weight of looper respectively and it is described as follows.

$$K_1(\theta) = 2Hbr\cos\theta\sin\theta \quad (24)$$

$$K_2(\theta) = 2\rho Hbg\frac{l}{\cos\beta}r\cos\theta \quad (25)$$

$$K_3(\theta) = W_L g r_L\cos\theta + \theta_G \quad (26)$$

J is moment of inertia in drive shaft of looper, θ is looper angle of rotation to the horizontal, σ is tension applied to the rolled material, T_{Lref} is reference of looper drive torque, H and b are strip thickness and strip width, ρ is specific gravity of rolled sheet, r is arm length of looper, l is half length between stands, W_L is looper molarity, $r_L$is distance from the rotation axis of looper to center of gravity, D is viscosity coefficient of friction in rotary shaft of looper, $\theta_G$is offset angle from looper angle θ of looper center of gravity, β is angle that lifts the rolling material from the horizontal, and the function of θ obtained from a geometrical relation respectively. It is assumed $\delta = 1$ when looper roll comes in contact with the rolling material, and $\delta = 0$ at noncontact.

The equations of dynamics in tension system are described as below.

$$\dot{\sigma} = \frac{E}{2l}\{1 + f(\sigma)V_R + \frac{\partial L}{\partial\theta}\dot{\theta}\} \quad (27)$$

$$\dot{V_R} = -\frac{1}{T_{ASR}}(V_R - V_{Rref}) \quad (28)$$

Here, V_R is work roll velocity, V_{Rref} is it's reference value of the velocity, $f(\sigma)$ is function of speed difference between stands, $L(\theta)$ is strip length between stands, E is Young's modulus of rolled material.

The jump phenomenon of looper angular velocity and tension caused when the mode shifts from contact

to noncontact are shown.

$$\dot{\theta}(t) = \epsilon_1 \dot{\theta}(t) \quad (29)$$

$$\delta(t) = \epsilon_2 \dot{\theta}(t) + \delta(t) \quad (30)$$

3.2.3 Mass Flow Rule

Mass flow rule is used in order to determine set value of rolling velocity. Mass flow rule can be described as follows.

$$h_1^o v_{R1}(1+f_1) = h_2^o v_{R2}(1+f_2) = h_3^o v_{R3}(1+f_3) \quad (31)$$

Where, h_i^o is the desired value of strip thickness at i^{th} stand.

3.2.4 Strip Thickness Control Agent

Gauge meter equation is described as below.

$$h = s + \frac{P}{M} \quad (32)$$

Where, h, s, P and M are exit strip thickness, roll gap, rolling force and mill modulus respectively. The control scheme of Gauge Meter AGC (Automatic Gauge Control) is given by

$$\Delta h_i = h_i - h_i^o \quad (33)$$

$$\Delta s_i = -k_i \Delta h_i \quad (34)$$

Where, k_i is AGC gain. AGC starts its operation when head end of strip arrives to the next stand.

3.2.5 Tension/Looper Control Agent

PID control is described as below.

$$m(t) = K_p\Big(e(t) + \frac{1}{T_i}\int e(t)dt + Td\frac{de(t)}{dt}\Big) \quad (35)$$

Where, m(t) is manipulated variable and in this case V_{Ri}, $e(t)$ is error and in this case looper deviation, K_p is proportional gain, T_i is integral time, and T_d is derivative time of PID control.

In simulator, PID control is carried out using looper angle model as follows.

$$\theta_i = \theta_i + \Delta\theta_i \quad (36)$$

$$\Delta\theta_i = K_p\Big\{(e_n - e_{n-1}) + \frac{T_s}{T_i}e_n + \frac{T_d}{T_s}(e_n - 2e_{n-1} + e_{n-2})\Big\} \quad (37)$$

Where, T_s is sampling time interval, e_n is error at sampling time nT_s, e_{n-1} is error at sampling time $(n-1)T_s$, and e_{n-2} is error at sampling time $(n-2)T_s$.

Tension algorithm is described as below.

$$\sigma_i = \sigma_i + \Delta\sigma_i \quad (38)$$

$$\Delta\sigma_i = K_p\Big\{(e_n - e_{n-1}) + \frac{T_s}{T_i}e_n\Big\} \quad (39)$$

$\Delta\sigma_i$ is described by the type of PI control equation.

3.3 Simulator for Hot Strip Mills

The simulator used in this paper consists of seven stands and six loopers between them. Simulation program for hot strip mills with controllers is stated below.

3.3.1 Interface

The agent based simulation model was applied, and the simulation of a hot strip control system was made. Displayed results of simulated dynamics of hot strip mills are shown in Fig.27. Time-series data of rolling mills and control systems are displayed as dynamic behaviors of hot strip mills. In addition, a dynamic simulator is made in three dimensions.

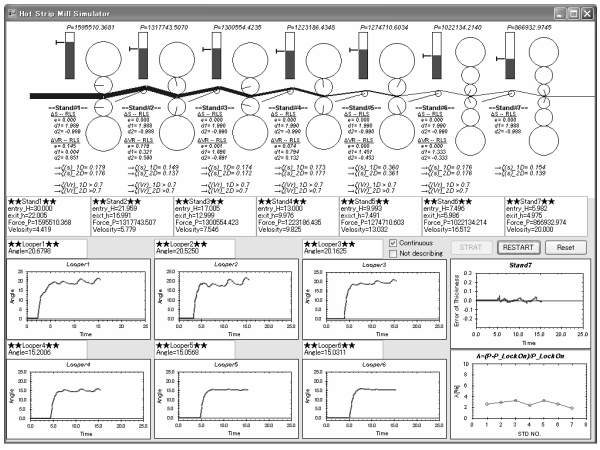

Fig. 27 Dynamic simulator

An example of displays of operating situation is shown in Fig.28. Each value of motor current, roll force, temperature, thickness, roll gap, and roll speed are displayed as rolling state. Moreover, the lower part display the time responses of temperature, shape, looper angle, and load balance.

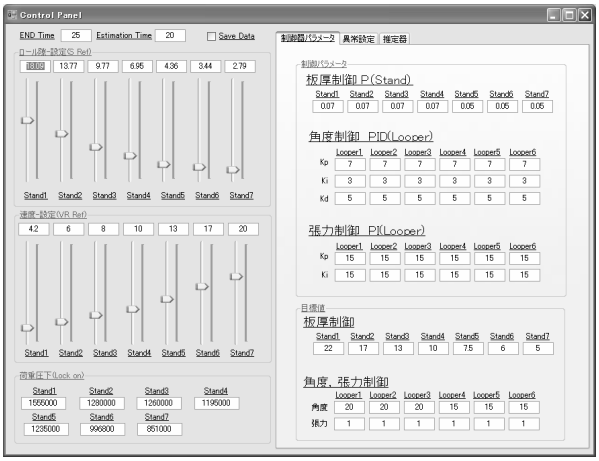

Fig. 28 Display part

3.3.2 Simulation of Rolling Characteristics

Using Eqs.(12) to (16) rolling force P is calculated. Then exit strip thickness h is calculated by Eq.(20). The method of the calculation is described in the flow chart of Fig.29. Table 5 summarizes the parameters used in the calculation.

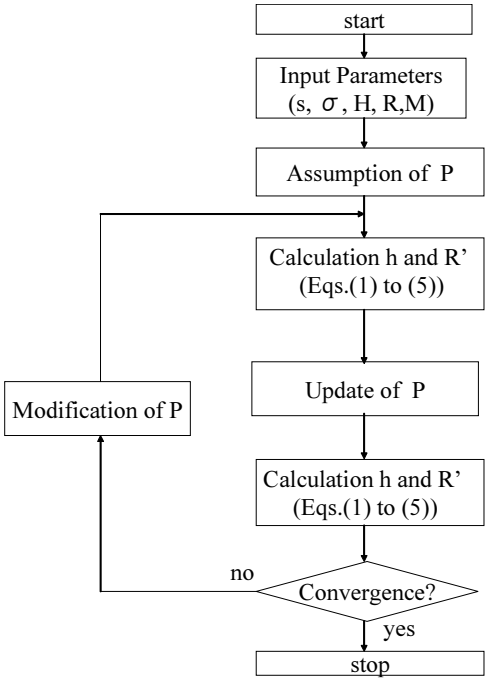

Fig. 29 Flow shart for calculation P

Table. 5 Simulation for calculation P

symbol	scale	meaning
M	400000[kgf/m^2]	Mill modulus
H_1	30[mm]	Entry thickness
R	400[mm]	Work roll radius
L	5.5[m]	Distans between stands
T_v	0.05[sec]	Time const of mill drive
T_s	0.05[sec]	Time const of gap set

3.3.3 Simulation of Inter Stands Looper Dynamics

Fig.30 shows seven stands hot strip mill system with controllers. The block diagram showing dynamic characteristics of inter stands looper are partially given as shown in Fig.31.

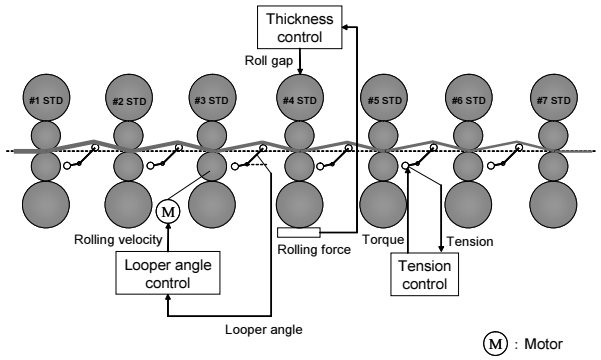

Fig. 30 Seven stands hot tandem mills

Firstly, rolling velocity and roll gap is determined as initial setting values. Where V_{R_7} is set at 20[m/s] and other rolling velocities are determined by mass flow rule, and initial setting value of roll gap s is calculated using aimed gage h^o, rolling force P and mill modulus M as follows. Where, i means stand number.

$$s_i = h_i^o - \frac{P_i}{M_i} \quad (i = 1 \sim 7) \tag{40}$$

When the strip arrives at 1st stand, rolling characteristics of the stand is started to calculate by flow in Fig.29, and AGC of 1st stand is started. After $\frac{L}{v_{f_1}}$[sec], the strip arrives at 2nd stand. Then rolling characteristics of the stand is started to calculate and the looper angle between 1st and 2nd stand is started to calculate. Then, looper control and AGC of 2nd stand are started. In the same way, after $\frac{L}{v_{f_2}}$[sec], the strip arrives at 3rd stand. Then rolling characteristics of the

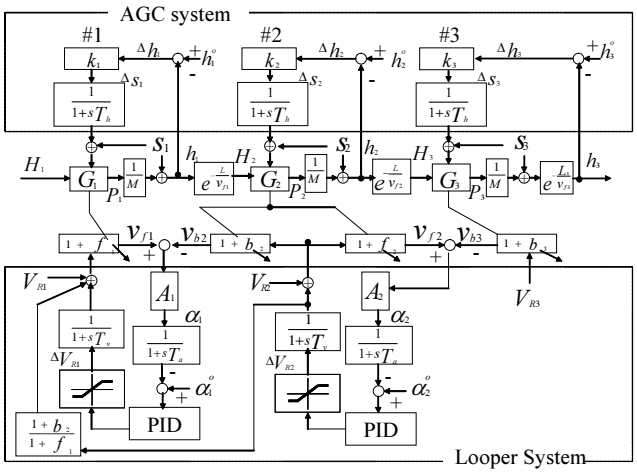

Fig. 31 Block diagram of mill control system

stand is started to be calculated and the looper angle between 2nd and 3rd stand start to move, accompanying with looper control and AGC of 3rd stand. Thus, it is calculated up to seven stands after 3rd stand.

Table 6 shows simulation parameters about base rolling condition.

Table. 6 Parameters for simulation

symbol	scale
W_L	1500[kg]
r	0.8[m]
D	0.00133[mm]
r_L	0.8[m]
l	2.25[m]
θ_c	0.1744[deg]
θ_G	0[deg]
θ_{acr}	0.05[m]

3.3.4 Numerical Experiment

The simulator used in this paper consists of seven stands and six loopers between them. Table 7 shows simulation parameters about basic roll schedule for mill setting, and Table 8 shows aimed values of looper angle and tension.

Where θ^o is desired a value of looper angle, h_1^o, h_2^o, h_3^o are desired values of strip thickness, σ^o is desired a value of tension.

The conditions for simulation are as follows. The total length of rolled material is 300[m], strip width of rolling material is 1000[mm], the distance between stands is 5.5[m] respectively. PID control was applied to looper angle and tension controls between stands. As for disturbance to rolling, change in flow stress of the deformed material K_{fm} is used. Fault diagnosis is one of the purposes of the simulator. After looper comes in contact with rolled material, flow stress change is set at 0.2[kgf/mm^2] as the magnitude of a squared wave. The simulation results are shown in Fig.32.

As shown in Fig.32, influenced results in strip thickness for each stand are observed. The influenced results in looper angles are also shown in Fig.32. Regardless of the disturbance, strip thicknesses and looper angles are regulated to their aimed values. However, oscillation waves induced by disturbance remain. Tension results between stands are also shown in Fig.32. It was confirmed that the tension converges to the aimed value after large tension is observed when looper comes in contact with rolling material.

3.4 Application to Diagnosis

3.4.1 Diagnostic System

Application of a dynamic simulator of hot strip mills to the diagnosis was carried out. Construction of diagnostic system is shown in Fig.33.

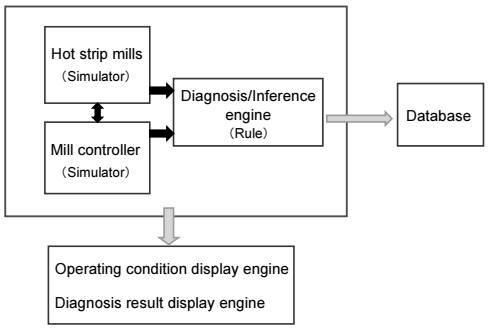

Fig. 33 Diagnostic system

As shown here, the operation support system is composed of hot strip mills, mill control system, inference engine for operation support, an operating condition display part, a diagnostic result displaying part, and a database. The agent based simulation model was applied to the hot rolling mills and the hot strip control system. The diagnostic part extracts the amount of variables by a fault through a dynamic simulator. Further the part generates rules from various situations. In

Table. 7 Simulation parameters of Mill system

Parameter	1 std.	2 std.	3 std.	4 std.	5 std.	6 std.	7 std.
h_i^o [mm]	22	17	13	10	7.5	6	5
s_i [mm]	18.09	13.71	9.77	6.95	4.36	3.44	2.79
$Reduction$ [-]	0.267	0.227	0.235	0.231	0.25	0.20	0.167
$Totalreduction$ [-]	0.267	0.433	0.567	0.667	0.75	0.80	0.833
K_{fm} [kgf/mm^2]	20.8	21.3	21.6	21.9	22.1	22.3	22.4
P_{i_0} [kgf]	1600000	1400000	1300000	1200000	1000000	1000000	1100000

Table. 8 Simulation parameters of Looper system

Parameter	1 lpr.	2 lpr.	3 lpr.	4 lpr.	5 lpr.	6 lpr.
θ_i^o [deg]	20	20	20	15	15	15
σ_i^o [kgf/mm^2]	1	1	1	1	1	1

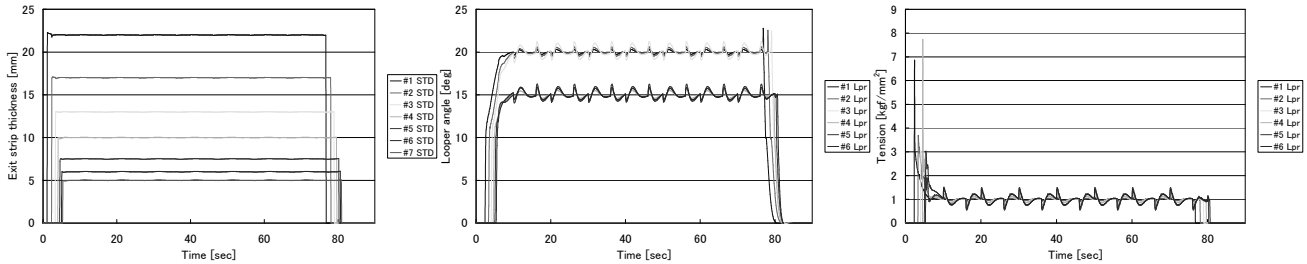

Fig. 32 Time change of rolling variables during rolling

combination of the simulator with the diagnostic part, simulation system has functions of diagnosis, prediction, and advice. The rules made in the diagnostic part are accumulated in the database. Data are used to visualize rolling phenomenon showing, diagnostic result, the reason in operating condition and diagnostic results which are illustrated in the displaying part.

3.4.2 Failure of Hot Strip Mills

As examples of failures, the following phenomena are assumed.

1. Deterioration of hydraulic circuit performance
2. New specification test material in rolling
3. Temperature variation induced by insufficient heating or partial cooling
4. Deterioration of mill drive system
5. Decrease in mill modulus of liner wear of mill stand
6. Temperature measurement error
7. Failure of strip shape by roll heat expansion and wear
8. Thickness and temperature variation, load in balance and failure of strip shape from setting of velocity and roll gap
9. Unstable rolling induced from excessive strip loop between stands by error setting
10. Failure of control system units

To reproduce these failures, mill setting is changed manually.

3.4.3 Numerical Experiment

To apply the simulator to the diagnosis, failures were made. In this time, error setting of roll gap was made. In the following, the effects of mill setting error of rolling conditions are shown, compared with nominal rolling shown in Fig.34. Here, Δs_i shows error from initial setting of i^{th} stand.

The threading time is united at 20[sec]. When a error setting is caused, non-stationary of initial rise in threading is important. It is summarized about the looper angle as shown in Table 9 as the results shown in Figs.35 to 39.

Symbol "+" shows large loop, and symbol "−" shows small loop, compared with threading of normal time shown in Fig.34. The number of symbol shows the level of loop change.

When s_2 was changed by error setting, the influence was confirmed to all looper. Especially, the feature is clearly shown in the 1st looper as shown Fig.35. The loop of 1st looper is small compared with that of normal time.

When s_4 was changed by error setting, it was confirmed that the loop of the 3rd looper becomes small. At the same time, it was oscillatory in the 4th looper and later as shown in Fig.36.

When s_7 was changed by error setting, it was confirmed that loop of the 6th looper is large. In addition, it is confirmed that the exit strip thickness is also affected by error setting in the final stand as shown in Fig.37.

When s_2 and s_3 were changed by error setting, it was different from the feature changing s_2. When s_2 was changed, loop of the 2nd looper was changed. However, when both s_2 and s_3 were changed, loop of the 2nd looper becomes small as shown in Fig.38.

In Fig.39, the feature when s_2 and s_4 were changed respectively was shown. In this case, loops from the 1st to the 3rd looper become small. At the same time, loop of the 4th looper becomes oscillatory.

As a result, when the error setting was caused in a stand, the loops of lower loopers are apt to become oscillatory. At the same time, it was confirmed that the loop of upstream looper becomes small it the roll gap of downstream stand is positive. And, oscillatory behavior was observed in the downstream loopers by the error setting.

These results means looper dynamics indicate errors in roll gap setting. The relations between error setting and looper dynamics are examples of rules for operation diagnosis.

4 CONCLUSION

In this paper, human support agent for design and diagnosis using classifier system was proposed. It was shown the system that can share information of database constructed by the design results and diagnosis results by experts. The classifier system was applied to analyze the data in the database and extract expert's knowledge. In this paper, the design of filter circuit was treated as an example of the design problem, and diagnosis of hot strip mills was treated as a example of the diagnosis problem.

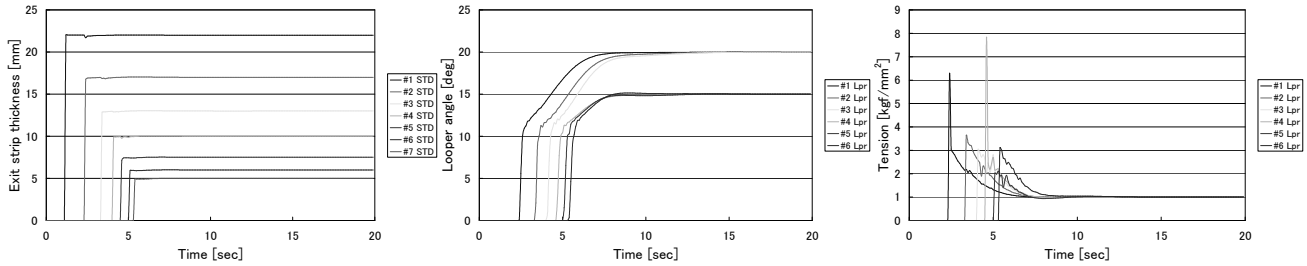

Fig. 34 Threading of normal time

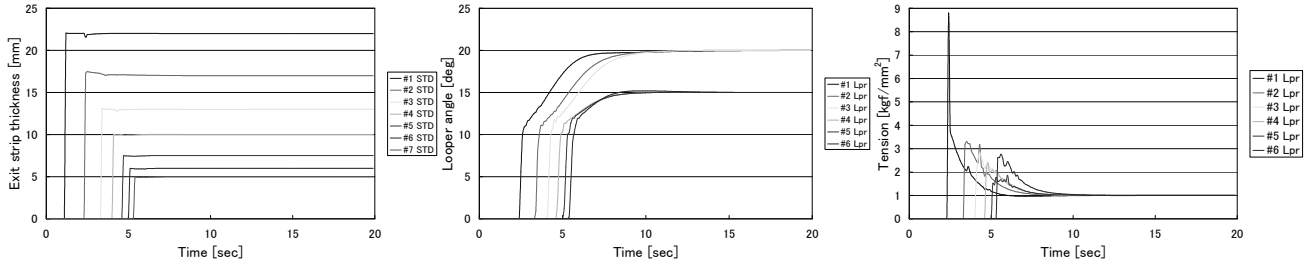

Fig. 35 Time change of thickness, looper angle and tension($\Delta s_2 = +1$[mm])

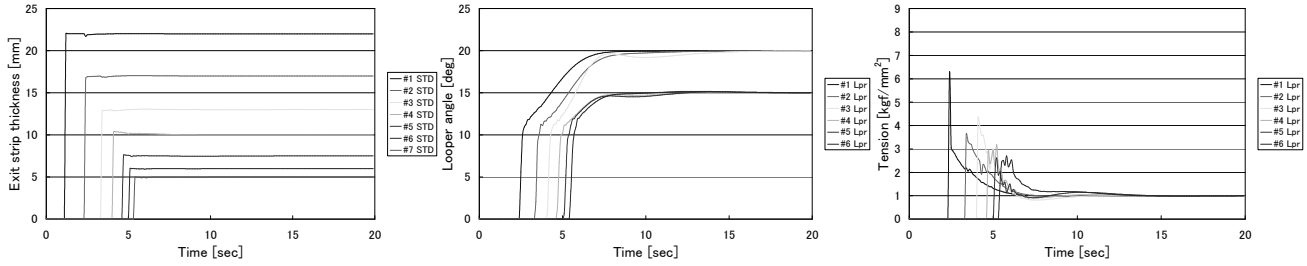

Fig. 36 Time change of thickness, looper angle and tension($\Delta s_4 = +1$[mm])

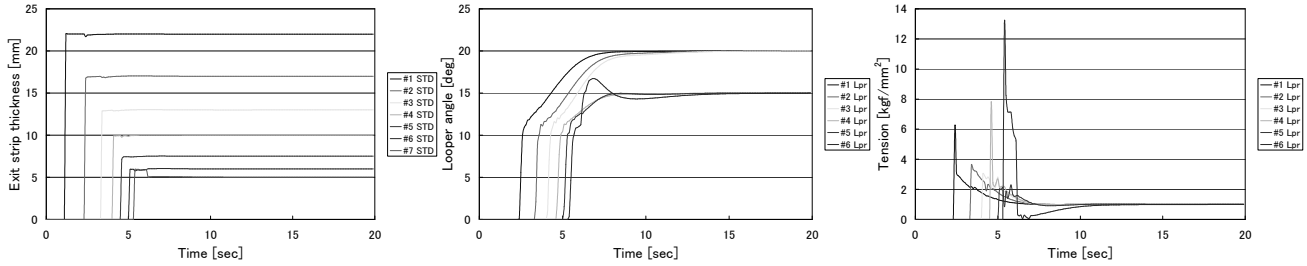

Fig. 37 Time change of thickness, looper angle and tension($\Delta s_7 = +1$[mm])

Table. 9 Looper system

Parameter	1 lpr.	2 lpr.	3 lpr.	4 lpr.	5 lpr.	6 lpr.
$\Delta s_2 = +1$ [mm]	$--$					
$\Delta s_4 = +1$ [mm]			$--$	$+-$	$+-$	$+-$
$\Delta s_7 = +1$ [mm]						$++$
$\Delta s_2, \Delta s_3 = +1$ [mm]	$--$	$--$				
$\Delta s_2, \Delta s_4 = +1$ [mm]	$--$	$--$	$--$	$+-$		

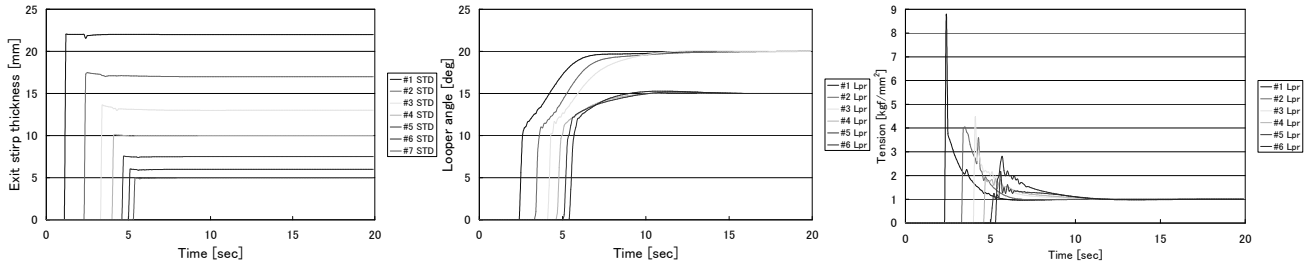

Fig. 38 Time change of thickness, looper angle and tension($\Delta s_2, \Delta s_3 = +1$[mm])

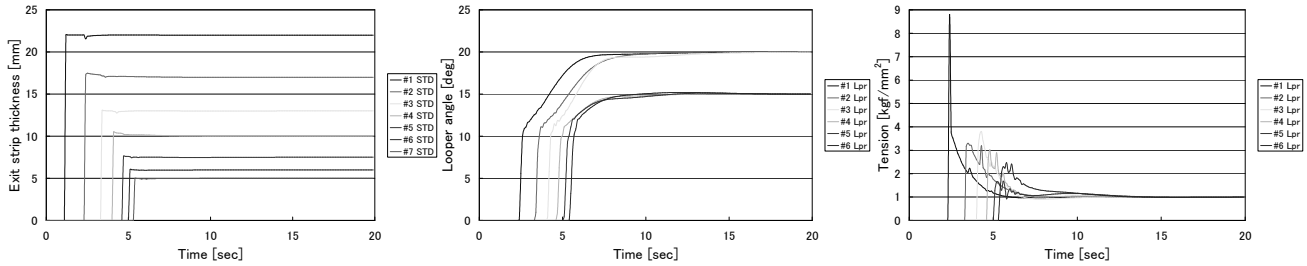

Fig. 39 Time change of thickness, looper angle and tension($\Delta s_2, \Delta s_4 = +1$[mm])

Classification system of circuit structures to support design was developed for practical use. This system consists of three functions, optimization, classification, and retrieval of the related database. Each function was checked through a numerical experiment. It was confirmed that the circuit satisfying with design specification was designed by optimization procedure. Possibility of classification of circuit structure was also shown. It was shown the use of database like presentment of design results and feedback of circuit information for efficiency of optimization.

For the diagnosis, agent based simulator for hot strip rolling mills with controllers was developed. Using the simulator, complex rolling phenomenon in roll contact zone and inter stands were successfully visualized. Further, the simulator was used to the operation diagnosis of a mill system. A complex rolling phenomenon of seven stand tandem mills was reproduced through the simulation. Effects of disturbance on rolling characteristics are discussed. It was confirmed that mill setting error greatly effects looper dynamics during threading.

REFERENCES

[1] Yuichi Yano, Toshiji Kato and Mitsunori Miki : Introductory Genetic Programming, Tokyo University Press (2001).

[2] Yuichi Yano, Toshiji Kato and Mitsunori Miki : International Journal of Control, (2004), 2208-2214.

[3] Lawrence Davis : Handbook of Genetic Algorithms, Reinhold, A Division of Wadsworth, Inc. (1990).

[4] R. M. M. Chen, P. C. K. Yu and A. M. Layfield : Proc. of the 1992 IEEE International Symposium on Circuits and Systems, (1992), 863-866.

[5] T. Kohonen : Self-Organizing Maps, Springer-Verlag Verlin Heidelverg, (1995).

[6] Satoru Kato, Kenta Koike, Tadashi Horiuchi : Transaction of EIS, (2005), 14-20.

[7] Azuma Ouchi, Masato Yamamoto and Hidenori Kawamura : Basic and Aplication of Multi Agent System -Computing Paradigm from Complex Systems Engineering-, Corona Publishing Co., Ltd., (2002).

[8] R. C. Baker and B. Charlie : ISIF International, (2003), 358-365.

[9] Kazuya Asano et al : IFCA, (2001), 319-324.

[10] Yoshihiro Abe et al : International Conference on Innovative Computing Information and Control 2006, (2006), 415-418.